

Analysis of the Oil Film in the Fluid-Static Pressure Spindle of a High-Speed Gear Shaping Machine Based on Fluid-Structure-Thermal Coupling

Zecheng Wang *

Tianjin University of Technology and Education, Tianjin, China

* Corresponding Author: Zecheng Wang

ABSTRACT

The optimisation of liquid hydrostatic spindle structural configurations and parameters constitutes a primary factor influencing the load-bearing capacity, oil film stiffness, and fluid temperature rise during high-speed cutting operations in gear shaping machines. To achieve high rigidity and precision while mitigating friction-induced temperature rise, advanced research is required into the influence of lubricant viscosity-temperature characteristics on the oil film properties of fluid dynamic spindles. Specifically, high-speed gear shaping machines exhibit an eccentric oil film effect in fluid dynamic bearings during high-speed cutting operations. Consequently, accurately investigating the motion patterns and characteristics of the radial surface in liquid-static spindles during practical theoretical design and engineering trials, while accounting for the impact of fluid temperature rise on cutting precision, remains a persistent research challenge.

KEYWORDS

High-speed Gear Shaping Machine; Hydrostatic Spindle; Oil Film Stiffness; Oil Film Temperature Rise; Thermal Deformation.

1. INTRODUCTION

In the field of precision machine tools, hydrostatic spindles have become the core component for achieving high-precision involute gear machining in high-speed gear shaping machines, owing to their exceptional motion accuracy, extremely high rigidity, outstanding damping characteristics, and exceptionally long service life[1]. However, these spindles face a critical fluid thermodynamic challenge in high-speed gear shaping machine applications: during the spindle's high-frequency reciprocating motion, viscous dissipation effects within the supporting oil film significantly intensify. The characteristics of hydrostatic spindles directly impact the machining efficiency, precision, and stability of the machine tool.

Viscous dissipation irreversibly converts the mechanical energy of spindle motion into thermal energy, causing the oil film temperature to rise sharply with increasing stroke speed (i.e., significant oil film temperature rise). This temperature increase triggers a series of severe performance degradations. Elevated temperatures lead to reduced lubricant viscosity, not only compromising spindle positioning accuracy but potentially causing it to lose load-bearing capacity. Localised high-temperature zones may induce thermal deformation in spindle and bearing structures, further deteriorating machining precision. Under extreme temperature surges, lubricant failure or transition to boundary lubrication may occur, substantially increasing the risk of adhesive wear or even seizure

(‘spinning shaft’) between the spindle and bearing surfaces. This can result in catastrophic equipment damage[2].

As one of the core issues in fluid mechanics, the precise analysis of bearing oil film characteristics consistently presents significant challenges. From a methodological perspective, the complexity of this problem manifests primarily in two aspects: firstly, at the theoretical analysis level, due to the intricate multiphysics coupling inherent in actual bearing operating conditions (including fluid-structure interaction, thermal effects, and surface roughness), classical lubrication theory based on the Reynolds equation struggles to yield closed-form analytical solutions; Secondly, in experimental research, the measurement of high-precision oil film parameters necessitates not only sophisticated testing systems (such as micrometre-level displacement sensors and high-speed camera equipment) but also entails substantial experimental costs and protracted testing cycles.

Traditional numerical solutions based on the Reynolds equation can provide preliminary predictions of bearing static and dynamic characteristics. However, their theoretical framework possesses inherent limitations: as a simplified form of the Navier-Stokes equations under specific assumptions, the Reynolds equation significantly reduces computational complexity by neglecting key factors such as fluid inertial effects, curvature influences, and three-dimensional flow characteristics. This simplification, however, comes at the cost of sacrificing the completeness of the physical model. This simplification may introduce non-negligible errors particularly under high-speed, heavy-load, or micro-scale operating conditions, thereby constraining the reliability of theoretical predictions. Qiang LI et al. employed a three-dimensional CFD approach to investigate the impact of journal misalignment on the transient flow characteristics of finite groove bearings, establishing a dynamic simulation framework for the bearing-rotor system that incorporates fluid-structure interaction (FSI)[3]. Minghui Guo et al. employed CFD techniques to numerically simulate six oil cavity configurations. Results demonstrated that CFD effectively reveals the correlation between oil cavity geometry and bearing static performance, with load-carrying capacity increasing with oil cavity circumference. An equilateral triangular oil cavity exhibited optimal performance, and simulation outcomes were experimentally validated for reliability[4]. Zhan Jinzhang et al. compared orifice and capillary throttling methods, finding that orifice throttling exhibits higher stiffness at low eccentricity ratios ($\varepsilon < 0.35$), while capillary throttling performs better at high eccentricity ratios[5]. Through fluid-structure interaction analysis, Yi Zongyu et al. observed that dynamic loads induced by high speeds cause periodic fluctuations in spindle eccentricity. A U-shaped oil cavity design enhances stiffness by 12.3% by increasing the effective bearing area[6]. Additionally, chamfering the oil cavity edges reduces stress concentration, though its contribution to stiffness improvement is limited at high speeds. Current research employs fluid-structure interaction analysis to investigate how spindle oil film characteristics affect bearing bushings. Increased stroke speeds may exacerbate spindle-bearing friction and cause significant lubricant temperature rise. Fedorynenko et al. observed through thermo-fluid coupling simulations that water-lubricated bearings exhibit uneven temperature distribution at high speeds due to fluid shear heating[7]. This induces thermal deformation, reducing oil film clearance and diminishing stiffness. Similarly, research by Yin Chengzhen et al. indicates that temperature rise in ultra-precision single-point diamond horizontal roller machine tool hydrostatic spindles correlates positively with rotational speed, hydraulic oil viscosity, and sealing oil edge length, while correlating negatively with oil supply pressure and oil film clearance[8]. Zhao Ziheng et al. observed that under ultra-high-speed conditions, the viscosity-temperature effect of lubricating oil causes strong coupling between the oil film pressure field and temperature field[9]. Although increased oil supply pressure intensifies flow and locally reduces temperature, elevated rotational speeds simultaneously amplify oil film pressure and temperature rise, diminishing actual load-bearing capacity due to elastic deformation of the bearing bush. Ma Wenqi et al. revealed through bidirectional fluid-structure interaction analysis that thermal elastic deformation of the bearing sleeve alters the spatial morphology of the air film/oil film, causing discrepancies between the designed thickness and the actual effective thickness[10]. This deformation further disturbs the oil film

pressure distribution, creating a vicious cycle of ‘thermal deformation – film thickness variation – reduced load-bearing capacity’.

Therefore, the author has selected a specific model of gear shaping machine as the subject of study. Based on the principles of hydrostatic bearing support, an analysis is conducted of the oil film characteristics and deformation of the spindle sleeve during the operational state of the high-speed gear shaping machine's spindle. Further analysis of the spindle's performance is achieved through fluid-structure interaction methods.

2. HYDROSTATIC SPINDLE OIL FILM PARAMETERS

Based on the three-dimensional modelling of a specific gear shaping machine spindle, the hydrostatic spindle structure is illustrated as shown. The hydrostatic spindle features four oil chambers, each connected to a throttle valve. Pressurised oil first flows through the throttle valve, where a pressure drop is generated before proceeding to the oil chamber and passing over the sealing lip. A hydrostatic oil film forms between the spindle and sleeve to bear radial loads. When the spindle is in its balanced position, the pressure within each oil chamber is equal, and the oil film thickness is uniform. During operation, radial loads cause the spindle to become eccentric, altering the pressure within each oil chamber and consequently changing the oil film thickness.

A schematic diagram of the gear shaping machine spindle structure is shown in Figure 1, with the spindle structural parameters listed in Table 1.

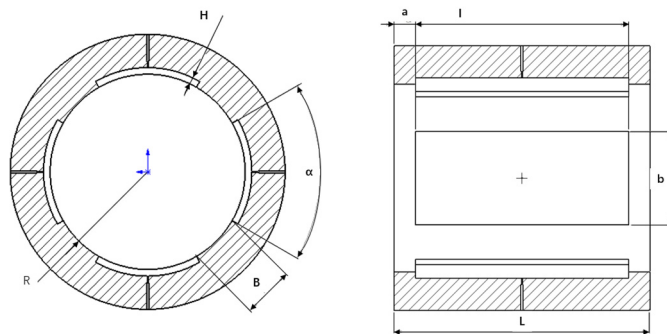


Figure 1. Schematic Diagram of the Gear Shaping Machine

Table 1. Spindle Structural Parameters

Parameter	Value
Static pressure spindle radius D/mm	44
Oil cavity width b/mm	46.1
Initial oil film clearance h_0/mm	0.02
Sealing edge length a/mm	10
Oil cavity depth H/mm	3
Sealing edge length B/mm	11.5
Spindle length L/mm	120
Half of the central angle enclosed by the oil cavity	30

3. LITERATURE REFERENCES

3.1. Liquid Hydrostatic Spindle Oil Film Boundary Condition Configuration

The liquid hydrostatic spindle provides support during machining operations. Initial research must analyse the structural parameters and operating conditions of the oil film to establish its overall

motion characteristics. Under stable conditions, oil is supplied uniformly via four circumferential ports. To maintain constant positive hydrostatic pressure and prevent pressure loss, a constant-pressure supply system is employed with $P_s = 1 \text{ MPa}$ to 3 MPa . The outer surface of the oil film is fixed to the bearing sleeve, while the inner surface is treated as a translational boundary connected to the spindle. Under the assumption of negligible slip, the spindle cutting speed ranges from 0 to 2 m/s. The bearing end face serves as the oil outlet connected to atmospheric pressure.

The control equations employ a second-order upwind discretisation scheme to solve for the oil film. To achieve rapid convergence, the discretisation algorithm utilised herein is SIMPLEC.

3.2. Fluid-Solid-Thermal Coupling Computation Process

The pressure field distribution and temperature field distribution of the oil film on the hobber spindle were calculated using Fluent. As Fluent software cannot perform coupled deformation analysis between fluid and solid components, this study employed the finite element software Workbench to import the lubricating oil film pressure field and temperature field results obtained from Fluent as loads into the solid model. This enabled a fluid-structure-thermal interaction analysis of the hydrostatic spindle in the gear shaping machine.

3.3. Tables

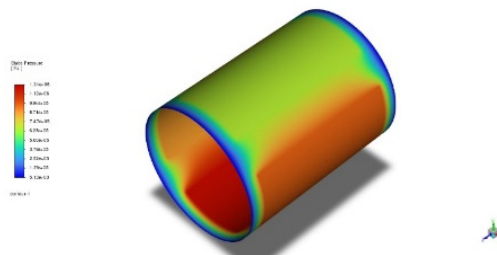


Figure 2. Oil Film of the Static Pressure Spindle

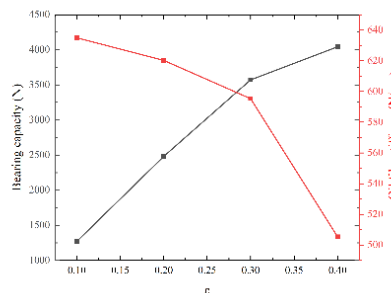


Figure 3. Oil film load-bearing capacity versus oil film pressure at different eccentricities

During machining operations, the hydrostatic spindle experiences transient fluctuations in radial cutting loads of varying magnitudes due to stroke motion and radial deflection. This induces a degree of eccentricity between the spindle shaft and sleeve under loaded conditions. The ratio of this eccentricity to the initial oil film thickness is termed the eccentricity ratio. As illustrated in the diagram, a higher eccentricity corresponds to greater pressure within the oil chamber on the eccentric side. When the eccentricity reaches 0.5, the oil film pressure is maximised. As the oil film eccentricity increases, so does the oil film pressure. As shown in Figure 2, the load-bearing capacity of the spindle oil film gradually increases with rising eccentricity, though the rate of increase gradually slows. At an eccentricity $\epsilon=0.5$, the oil film load-bearing capacity is approximately four times that observed at $\epsilon=0.1$. At low eccentricity ratios, the oil film thickness is relatively uniform, the pressure gradient is stable, and the oil film stiffness is strong. As the eccentricity ratio increases, the oil film thickness

decreases and the oil film stiffness diminishes. Specifically, at an eccentricity ratio $\varepsilon = 0.1$, the oil film stiffness is 0.8 times that at an eccentricity ratio $\varepsilon = 0.5$.

3.4. Spindle Oil Film Analysis

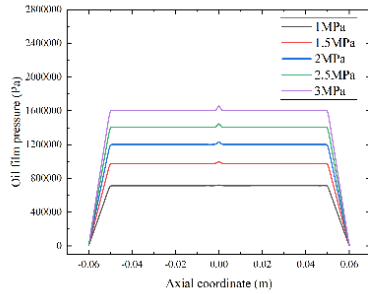


Figure 4. Oil film pressure distribution under different oil supply pressures

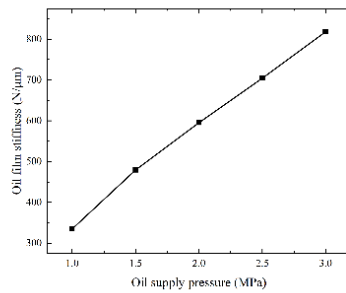


Figure 5. Oil film stiffness at different oil supply pressures

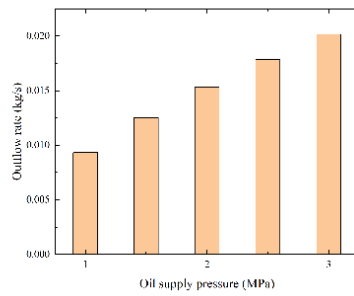


Figure 6. Outlet flow rate at different supply pressures

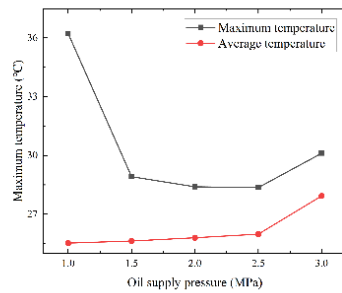


Figure 7. Oil film temperature rise under different oil supply pressures

During spindle operation, the oil film undergoes localised temperature rise due to compression and friction forces acting upon it. Consequently, the effects of oil supply pressure and stroke velocity on the pressure and temperature fields within the fluid domain are analysed.

As shown in Figures 4 to 7, when the eccentricity $\varepsilon = 0.3$, the thinnest point of the oil film measures $14 \mu\text{m}$. The pressure on the thinnest side of the oil film increases with rising supply pressure. The greater the pressure gradient formed within the film, the stronger the oil film's resistance to external loads (i.e., its stiffness). The oil film outlet flow rate increases with rising supply pressure. Given the reduced oil film thickness at the sealing edge, shear forces concentrate on the axial sealing surface. Consequently, temperature rise is primarily localised at the sealing surface, with the highest temperature occurring at the thinnest point on the axial sealing surface. Thus, the influence of viscous heating on the local temperature distribution within the spindle oil film must be considered. At low supply pressures, reduced oil film pressure diminishes the spindle outlet flow rate. Consequently, less heat is dissipated from the spindle region via the oil, leading to elevated oil film temperatures. Increasing the supply pressure markedly reduces the maximum temperature generated within the oil film. However, as supply pressure further increases, the spindle outlet flow rate rises significantly. The heat generated by oil film shear forces then substantially exceeds the heat dissipated by the oil. This results in a slight increase in the maximum oil film temperature and a rise in the overall average temperature of the oil film.

Based on actual operating parameters, a fluid simulation model was established to investigate the effects of non-lubricating oil pressure ($P = 1 \text{ MPa} - 3 \text{ MPa}$) on the spindle oil film pressure and oil film temperature rise. As shown in Figure 8, when the oil supply pressure $P_s = 1 \text{ MPa}$, the maximum oil film temperature is [value omitted]. When $P_s = 3 \text{ MPa}$, the maximum oil film temperature is [value omitted]. Considering the significant impact of temperature on spindle sleeve deformation, subsequent analysis will examine the extent of spindle deformation influenced by the oil film.

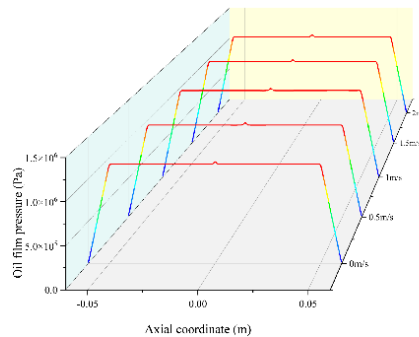


Figure 8. Oil film pressure distribution at different stroke speeds

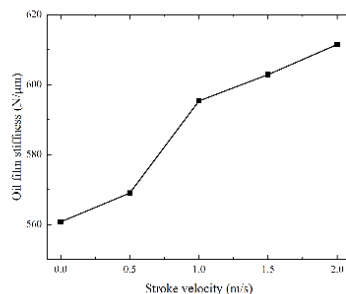


Figure 9. Oil film stiffness at different stroke speeds

Further analysis examines the impact of spindle stroke velocity on the spindle oil film. As depicted in Figures 9 and 10, increasing spindle stroke velocity causes slight variations in oil film pressure while enhancing oil film stiffness. With rising stroke velocity, flow rate at the spindle's forward-side outlet increases, while flow at the reverse-side outlet decreases, with overall outlet flow remaining

largely constant. As the instantaneous spindle stroke velocity increases, heat generated by oil film shear notably rises, leading to a significant increase in oil film temperature and an elevated average film temperature. Considering the increased stroke velocity, the higher flow rate at the forward outlet carries away more heat via the oil flow. Consequently, the maximum oil film temperature occurs at the reverse sealing surface, with this peak temperature increasing markedly as stroke velocity rises. As illustrated in Figure 11, a fluid simulation model was established based on actual operating parameters to investigate the effects of stroke velocity ($V = 0 \text{ m/s}$ to 2 m/s) on spindle oil film pressure and temperature rise. At stroke velocity $V=1 \text{ m/s}$, the maximum oil film temperature is [value omitted]. At stroke velocity $V=2 \text{ m/s}$, the maximum oil film temperature is [value omitted]. As stroke velocity increases, the oil film temperature rise markedly increases, significantly affecting the deformation of the spindle sleeve. To prevent spindle deformation, a fluid-structure-thermal coupling analysis was conducted to investigate the magnitude of spindle deformation influenced by the oil film.

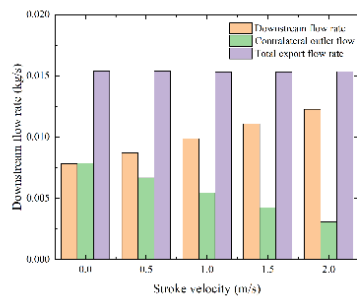


Figure 10. Outlet flow rate at different stroke speeds

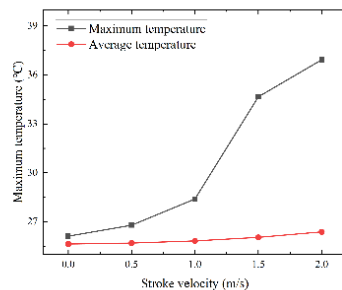


Figure 11. Oil film temperature rise at different stroke speeds

Color figures are welcome for the online version of the journal. Generally, these figures will be reduced to black and white for the print version. Authors should indicate on the checklist if they wish to have them printed in full color and make the necessary payments in advance.

3.5. Deformation Analysis of Spindle Bushings

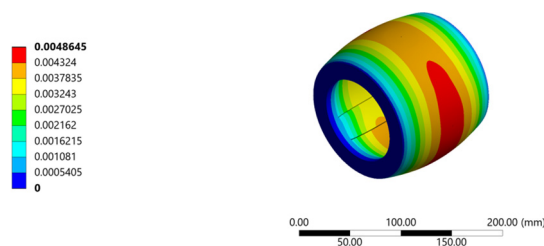


Figure 12. Deformation contour plot of the spindle bushing

Apply fixed constraints to the hobber spindle sleeve. Set the oil film thickness to $20\mu\text{m}$, inlet oil temperature to 25°C , and stroke velocity to 1m/s . Import the pressure and temperature fields obtained from the Fluent software as loads into the finite element model of the hobber spindle sleeve. The simulation calculates the deformation field of the sleeve.

As shown in Figure 12, the maximum deformation of the bearing sleeve is 0.00468 mm , while the minimum variation in oil film thickness is 0.00387 mm . The greatest deformation of the bearing sleeve occurs in the oil chamber on the side of the thinnest oil film and on portions of the axial sealing surface.

Considering the oil film lubrication characteristics of the gear shaping machine spindle, the bearing surface directly contacts the oil film surface. Consequently, variations in the oil film's pressure and temperature fields exert direct effects upon the bearing. Focusing solely on the influence of the oil film flow field on the spindle bearing, the deformation results are analysed under the combined effects of fluid-structure interaction and thermal coupling.

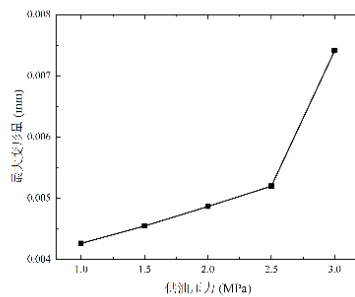


Figure 13. Maximum deformation of the bearing sleeve under different oil supply pressures

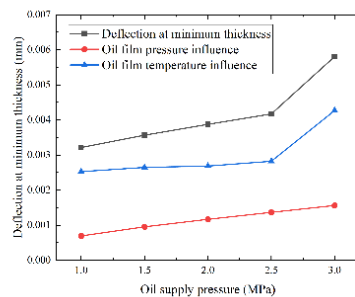


Figure 14. Deformation at the minimum oil film thickness under different oil supply pressures

Analyse the deformation of the bearing sleeve based on the influence of supply pressure on the oil film pressure field and temperature field. As illustrated in Figure 13 and 14, with increasing oil supply pressure, the load exerted by the oil film on the bearing sleeve grows, leading to a gradual increase in the maximum deformation of the sleeve. Notably, when the oil supply pressure rises to 2.5 MPa , the deformation of the sleeve increases dramatically. Meanwhile, the variation in the minimum oil film thickness between the spindle and the sleeve increases with rising oil supply pressure. Analysis of the temperature and pressure fields indicates that the variation in minimum oil film thickness is primarily influenced by the pressure field.

Further analysis of the influence of spindle stroke velocity reveals, as shown in Figures 15 and 16, that both oil film pressure and oil film temperature increase with rising spindle stroke velocity. Considering fluid-structure thermal coupling effects, the sleeve is directly subjected to the fluid pressure field and temperature field acting upon its surface. The overall deformation of the bearing sleeve increases with higher stroke speeds. When speeds are below 0.5 m/s , deformation remains relatively small; however, as speed increases further, the overall deformation of the bearing sleeve rises sharply. Considering the deformation at the minimum oil film thickness between the spindle and

sleeve, the figure indicates that deformation increases gradually at low speeds. As speed increases, deformation at the minimum oil film thickness becomes markedly greater. The effects of the pressure field and temperature field on deformation are examined separately. Deformation at the minimum oil film thickness is less influenced by the pressure field but significantly affected by the temperature field.

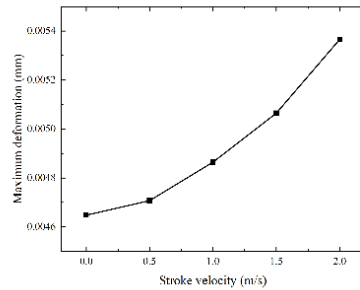


Figure 15. Maximum deformation of the bearing sleeve at different stroke speeds

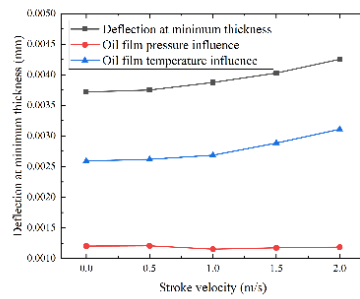


Figure 16. Deformation at the minimum oil film thickness under different stroke speeds

4. SUMMARY

The supply pressure directly influences the pressure, stiffness, and flow rate of the spindle oil film. Its effect on oil film temperature—particularly the maximum temperature at the thinnest sealing surface—is non-linear: both excessively low and excessively high pressures can cause temperature rise issues. A critical supply pressure point exists where the maximum temperature is minimised. Whilst continuously increasing supply pressure can boost flow to dissipate more heat, the friction-induced heating effect ultimately prevails, leading to an overall rise in the average oil film temperature.

Increasing the spindle stroke velocity slightly elevates oil film pressure and stiffness, alters flow distribution (increasing in the forward direction and decreasing in the reverse direction while maintaining total volume), and causes a significant rise in oil film temperature (particularly with a dramatic increase in maximum temperature at the reverse-side sealing surface). Simulation data confirms the severe temperature rise resulting from increased velocity. To prevent resulting sleeve deformation, fluid-structure-thermal coupling analysis must be conducted to quantify spindle deformation.

CONFLICTS OF INTEREST

The authors declare that they have no conflict of interest.

ACKNOWLEDGMENTS

This is the place to fill in information about funds, sponsors, etc. that need to be thanked.

REFERENCES

- [1] Xiong Wanli, Hou Zhiquan, Lü Lang, Yang Xuebing, Yuan Julong. A Method for Calculating the Stiffness and Damping of Liquid Dynamic and Static Pressure Bearings Based on the Moving Mesh Model [J]. Transactions of the Chinese Society of Mechanical Engineering, 2012, 48(23): 118-126.
- [2] WANG Lili, YUAN Guoteng, GENG Huan, Ling Peng. Analysis of the effect of viscosity-temperature effect of Lubricating Oil on the per-formance of hybrid bearing[J]. Lubrication Engineering,2020,45(1): 54-58.
- [3] Li Q, Liu S L, Pan X H, et al. A new method for studying the 3D transient flow of misaligned journal bearings in flexible rotor-bearing systems[J]. Journal of Zhejiang University-Science A (Applied Physics & Engineering), 2012, 13 (04): 293-310. K. Elissa, "Title of paper if known," unpublished.
- [4] Guo M, Tian Z, Feng X, et al. CFD-based method for hydrostatic bearings performance: static characteristics with various recess shapes[J]. International Journal of Hydromechanics,2024,7(2):176-192.
- [5] ZHAN Jinzhang, YIN Zhiqiang, HU Chengwu, XIE Jing. Analysis on bearing characteristics of hydrostatic support under different throttling modes [J]. Lubrication Engineering, 2025. Lubrication Engineering, 2025, 50(4): 58-64. M. Young, The Technical Writer's Handbook. Mill Valley, CA: University Science, 1989.
- [6] YI Zongyu, DING Guolong, WANG Wei, PENG Ling. Optimisation design of hydrostatic pressure spindle structure for gears Based on Fluid-Structure Interaction [J]. Machine Tool & Hydraulics, 2023, 51(13): 87-94.
- [7] Fedorynenko D, Kirigaya R, Nakao Y. Dynamic characteristics of spindle with water-lubricated hydrostatic bearings for ultra-precision machine tools[J]. Precision Engineering,2020,63(prepublish):187-196.
- [8] YIN Chengzhen, ZHANG Lianxin, WANG Baorui, et al. Multi-physical field coupling simulation and experimental study on thermal characteristics of hydrostatic spindle[J]. Lubrication Engineering,2019,44(9): 126-135.
- [9] ZHAO Ziheng, TAN Yanqing, MA Lianjie, XU Pengyang. Study of oil film characteristics of ultra -high speed liquid hybrid bearings considering Fluid-Solid Coupling Effect[J]. Lubrication Engineering, 2024, 49(7): 50-57.
- [10] Ma Wenqi, Ma Hailong, Qin Yubin, Huang Dali. Analysis of Bidirectional Fluid-Structure Interaction Characteristics in Gas Bearing-Rotor Systems and Establishment and Validation of Equivalent Gas Film Thickness [J]. Journal of South China University of Technology (Natural Science Edition), 1-8.